Trinuclear Palladium(II) Complexes with 2-Hydroxy-4-methoxyacetophenone N^4-Dimethylthiosemicarbazone: Synthesis, Spectral Studies and Crystal Structure of a Tripalladium Complex

Dimitra Kovala-Demertzi,*[a] Nikolaos Kourkoumelis,[a] Mavroudis A. Demertzis,[a] John R. Miller,[b] Christopher S. Frampton,[c] John K. Swearingen,[d] and Douglas X. West[d]

Keywords: Palladium / S ligands / One-dimensional extended networks / Structure elucidation

The synthesis and spectral characterization of a new *triangular,* trinuclear palladium(II) complex with the dianion of 2-hydroxy-4-methoxyacetophenone N^4-dimethylthiosemicarbazone, 4MeOAp4Me$_2^{2-}$ is reported. The X-ray crystal structure determination of [Pd(4MeOAp4Me$_2$)]$_3$·DMSO shows it to contain a chair-type hexagon of alternating Pd and S atoms which form a molecular bowl. The crystal structure of $H_2$4MeOAp4Me$_2$ shows that it is the *E* isomer with respect to the imine bond of the thiosemicarbazone moiety.

Introduction

Metallic palladium, and its mononuclear and trinuclear palladium(II) compounds, are the catalysts of choice for many reactions.[1] For example, palladium acetate is employed as a homogeneous catalyst in a large number of organic syntheses.[2] Palladium acetate, $Pd_3(\mu\text{-}OAc)_6$, is trinuclear with a triangular arrangement of nonbonded palladium atoms,[3a] and $[Pd_3(\mu\text{-}O_2CMe)_3(\mu\text{-}MeSCHR)_3]$[3b] is a mixed-sphere palladium complex in which the solid state nuclearity and the palladium acetate structure are retained. The structures of both triangular and linear trinuclear palladium(II) complexes have been determined.[3]

Thiosemicarbazones of salicylaldehyde and 2-hydroxyacetophenone have recently attracted considerable attention because of their potential biological properties[4] and catalytic activity.[5] Binuclear copper(II)[6] and nickel(II)[7] complexes of these N^4-substituted thiosemicarbazones have phenoxide bridges. Recently, a trinuclear palladium complex[8] with sulfur bridges, and a trinuclear nickel(II) complex with both Ni–O,O–Ni and Ni–S,O–Ni bridging patterns have been reported.[9] Palladium(II) complexes of 2-formylpyridine, 2-acetylpyridine and 2-benzoylpyridine N^4-substituted thiosemicarbazones have also been studied with regard to their structural and biological properties, and some of them have shown remarkable antitumor activity.[10] Therefore we decided to expand our studies of palladium(II) complexes to include other potentially tridentate thiosemicarbazone ligands and report here the structure of [Pd(4MeOAp4Me$_2$)]$_3$·DMSO (where 4MeOAp4Me$_2$ is the dianion of 2-hydroxy-4-methoxyacetophenone N^4-dimethylthiosemicarbazone), which has Pd–S–Pd bridging. Also included is the crystal structure of the uncomplexed 2-hydroxy-4-methoxyacetophenone N^4-dimethylthiosemicarbazone, $H_2$4MeOAp4Me$_2$.

[a] Department of Chemistry, University of Ioannina, 45110 Ioannina, Greece
E-mail: dkovala@cc.uoi.gr
[b] Department of Biological and Chemical Sciences, University of Essex, Wivenhoe Park, Colchester CO4 3SQ, United Kingdom
[c] Roche Discovery Welwyn, Welwyn Garden City, Hertfordshire AL7 3AY, United Kingdom
[d] Department of Chemistry, Illinois State University, Normal, IL 61790-4160, USA

Results and Discussion

The negative charge distribution on the atoms in a molecule with several donor centers can be used to study the formation of donor-acceptor bonds with a metal. From our

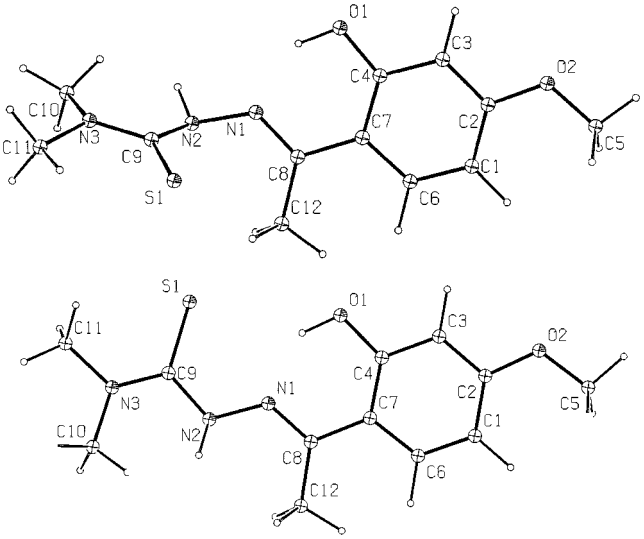

Figure 1. The fully PM3-optimized geometry of the neutral $H_2$4MeOAp4Me$_2$ molecule in the gas phase (a: top) and in methanol (b: bottom); the numbering used in the body of the text is applied

  1434–1948/00/0404–0727 $ 17.50+.50/0

Table 1. The calculated charges, electron densities, ionization potentials, dipole moments and ΔH_f (kcal/mol) for $H_2$4MeOAp4Me$_2$, H_2L, and the dianion 4MeOAp4Me$_2^{2-}$, L^{2-}; atom numbers are in accord with the notation of Figure 1

Atom	Charge[a][b] $H_2$4MeOAp4Me$_2$	Electron densities	Charge[b][c] $H_2$4MeOAp4Me$_2$	Electron densities
O1	–0.258	6.257	–0.333	6.333
O2	–0.184	6.184	–0.231	6.231
N1	–0.261	5.262	–0.238	5.238
N2	0.089	4.911	0.142	4.858
N3	0.075	4.925	0.293	4.707
S	–0.318	6.318	–0.711	6.711
	Charge[a][d] 4MeOAp4Me$_2^2$	Electron densities	Charge[c][d] 4MeOAp4Me$_2^{2-}$	Electron densities
O1	–0.563	6.563	–0.755	6.755
O2	–0.229	6.229	–0.244	6.244
N1	–0.066	5.066	–0.209	5.209
N2	–0.244	5.244	–0.203	5.203
N3	–0.029	5.029	–0.028	5.028
S1	–0.699	6.699	–0.918	6.918

[a] In the gas phase. – [b] The dipole moment and the ΔH_f are 4.62 Debye and 1.90 kcal/mol and 15.82 Debye and –24.97 kcal/mol for $H_2$4MeOAp4Me$_2$ in the gas state and in methanol, respectively. – [c] In CH_3OH. – [d] The dipole moment and the ΔH_f are 3.12 Debye and –17.88 kcal/mol and 7.43 Debye) and –223.65 kcal/mol for 4MeOAp4Me$_2^{2-}$ in the gas state and in methanol, respectively.

results the sulfur atom with maximum electron density and negative charge is predicted to be the preferred metal binding site; this agrees with the structural studies. The high effective charge and the high electron density value for the phenolic oxygen O1 and the imine nitrogen N1, also indicate strong electron-donor properties. The effective charges on the nitrogen atoms explain the conjugation of the thiosemicarbazonato moiety. The calculated molecular structures of the neutral $H_2$4MeOAp4Me$_2$ both in the gas phase and methanol are shown in Figure 1. The optimized geometry in methanol is *ZEZ* and is similar to that observed by X-ray diffraction for $H_2$4MeOAp4Me$_2$, the differences being attributable to packing effects. The data in Table 1 show the charge, electron densities for the various atoms, ionization potential, total dipole moment and enthalpy of formation of neutral $H_2$4MeOAp4Me$_2$ and the dianion 4MeOAp4Me$_2^{2-}$, in the gaseous state and in methanol, that have been calculated using MOPAC93.[11] As is evident from these data, the configuration in methanol is the preferred one over the configuration in the gas phase for $H_2$4MeOAp4Me$_2$ and 4MeOAp4Me$_2^{2-}$. The values obtained in methanol solution can be considered as a good approximation of the relative stability of the species in CH_3OH/H_2O. For 4MeOAp4Me$_2^{2-}$ a dramatic difference in stability is seen in methanol and in other polar solvents. The relative stability was computed as 23 and 206 kcal.mol^{-1} for the neutral and dianionic species, respectively.

The interaction of K_2PdCl_4 with $H_2$4MeOAp4Me$_2$ in basic solution (aqueous methanolic ammonia, pH ≈ 9) afforded the trinuclear complexes **1**, **2** and **3** according to the reactions:

$$K_2PdCl_4 \text{ with } H_2\text{4MeOAp4Me}_2 \longrightarrow [Pd(\text{4MeOAp4Me}_2)]_3 \cdot 3\,H_2O\ (\mathbf{1}) + 6\,KCl + 6\,HCl \quad (1)$$

$$\mathbf{1} \longrightarrow [Pd(\text{4MeOAp4Me}_2)]_3\ (\mathbf{2}) + 3\,H_2O \quad (2)$$

$$\mathbf{2} + DMSO \longrightarrow [Pd(\text{4MeOAp4Me}_2)]_3 \cdot DMSO\ (\mathbf{3}) \quad (3)$$

The stoichiometry of the complexes indicates that palladium(II) is coordinated by the doubly charged anion 4MeOAp4Me$_2^{2-}$ formed on the loss of the two protons from the phenolic oxygen and thioamide nitrogen, N2.

Molecular Structures

The structure of the uncomplexed thiosemicarbazone, $H_2$4MeOAp4Me$_2$, with two crystallographically different molecules per unit cell is shown in Figure 2 and the crystallographic data in Table 2, the bond lengths in Table 3 and bond angles in Table 4. The ligand has a *ZEZ* configuration about the bonds C1–C2, N1–C7 and N2–C8. N2H (and N5H) form an intermolecular hydrogen bond to a thione sulfur of an adjacent molecule, and the N2H (and N5H) groups of this molecule form hydrogen bonds to the sulfur atom of the first molecule, resulting in a dimer analogous to the dimer found for a number of heterocyclic thioureas.[12] The crystal packing is stabilized by intermolecular hydrogen bonds of the type C–H···O, O(3a)···H–C(2),[13] and by intramolecular hydrogen bonds. O1H and O3H form bifurcated intramolecular hydrogen bonds with their imine nitrogens, N1 and N3, and sulfur atoms, S1 and S2,

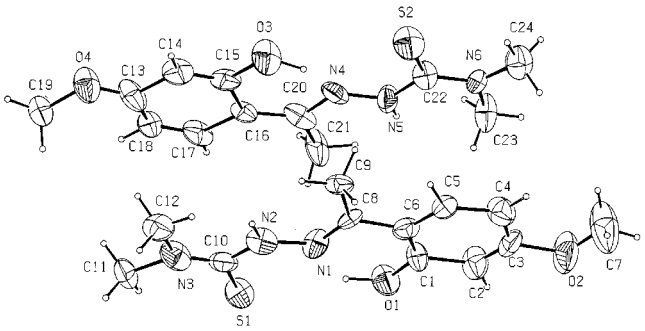

Figure 2. A perspective view of the two crystallographic different molecules of $H_2$4MeOAp4Me$_2$ (atoms at 50% probability)

Table 2. Crystal data and structure refinement for $H_2$4MeOAp4Me$_2$ and [Pd(4MeOAp4Me$_2$)]$_3$·DMSO

Empirical formula	$C_{12}H_{17}N_3O_2S$	$C_{36}H_{45}N_9O_6Pd_3S_3·C_2H_6OS$
Molecular mass	267.3	1193.40
Crystal system	Triclinic	Triclinic
Space group	*P*1 (# 1)	*P*–1 (# 2)
a, Å	8.119(4)	10.2412(1)
b, Å	9.064(2)	12.9971(2)
c, Å	9.629(2)	18.8397(2)
α, °	100.43(2)	92.6569(2)
β, °	101.67(3)	101.0277(7)
γ, °	96.33(3)	109.5790(8)
V, Å^3	674.6(8)	2302.45(5)
Z	2	2
D(calcd.), g cm^{-3}	1.316	1.721
F(000)	284	1200
μ(Mo-K_α), cm^{-1}	2.39	14.0
Crystal size, mm	0.10 × 0.15 × 0.30	0.02 × 0.04 × 0.40
Temperature, K	293(2)	123
λ(Mo-K_α)	0.71073	0.71073
φ min–max, °	1.0–26.38	1.1–26.4
hkl range	0, 10; –11, 11; –12, 12	–12, 12; –16, 16; –23, 23
Total, unique data, *R*(int)	3449, 3317	22641, 9234, 0.035
Observed data	1848 [$I > 3.0\ \sigma(I)$]	7425 [$I > 2.0\ \sigma(I)$]
N(ref), *N*(par)	3317, 330	9244, 564
R, *wR*	0.044, 0.099	0.0387, 0.1051
Goodness-of-fit on F^2	0.628	1.01
Largest diff. peak/hole, eÅ^{-3}	0.52/–0.32	0.81/0.79

Table 3. Selected bond lengths (Å) for $H_2$4MeOAp4Me$_2$ and [Pd(4MeOAp4Me$_2$)]$_3$·DMSO

$H_2$4MeOAp4Me$_2$		[Pd(4MeOAp4Me$_2$)]$_3$·DMSO	
S1–C10	1.65(2)	S1–C10	1.800(6)
N3–C10	1.29(3)	N3–C10	1.358(6)
N2–C10	1.39(2)	N2–C10	1.309(7)
N1–N2	1.39(2)	N1–N2	1.401(5)
N1–C8	1.26(2)	N1–C8	1.316(6)
C1–O1	1.32(2)	C1–O1	1.323(5)
C3–O2	1.48(3)	C3–O2	1.369(6)
S2–C22	1.71(2)	S2–C22	1.821(4)
N6–C22	1.37(2)	N6–C22	1.362(6)
N5–C22	1.36(2)	N5–C22	1.275(6)
N4–N5	1.38(2)	N4–N5	1.406(6)
N4–C20	1.32(2)	N4–C20	1.316(6)
C13–O4	1.25(2)	C13–O3	1.314(5)
C15–O3	1.40(2)	C15–O4	1.373(7)
		S3–C34	1.794(5)
		N9–C34	1.356(5)
		N8–C34	1.306(6)
		N7–N8	1.419(5)
		N7–C32	1.334(6)
		C25–O5	1.322(6)
		C27–O6	1.370(7)
		Pd1–S1	2.2585(12)
		Pd1–S3	2.3347(13)
		Pd2–S1	2.3578(12)
		Pd2–S2	2.2713(12)
		Pd3–S2	2.3579(12)
		Pd3–S3	2.2536(13)
		Pd1–O1	2.000(3)
		Pd1–N1	2.012(4)
		Pd2–O3	1.987(4)
		Pd2–N4	2.004(4)
		Pd3–O5	1.997(3)
		Pd3–N7	2.004(4)

respectively. The various distances and angles for the intramolecular and intermolecular hydrogen bonding of both forms of $H_2$4MeOAp$_4$Me$_2$ are listed in Table 5.

The two crystallographical forms of the $H_2$4MeOAp$_4$Me$_2$ molecules have the greatest differences in the following bond lengths in the thiosemicarbazone moieties: S1–C10, 1.65(2) Å and S2–C22, 1.71(2) Å; N3–C10, 1.29(3) Å and N6–C22, 1.37(2) Å; and N1–C8, 1.27(2) Å and N4–C20, 1.32(2) Å. The bond angles in the thiosemicarbazone moieties having the greatest differences are N3–C10–S1, 126.6(12)° and N6–C22–S2, 122.2(11)°; N1–N2–C10, 121.4(12)° and N4–N5–C22, 116.8(13)° and C8–N1–N2, 121.1(11)° and C20–N4–N5, 115.4(13)°. The phenoxy and methoxy bond lengths and angles are also significantly different suggesting that the differences in the two $H_2$4MeOAp4Me$_2$ molecules are due to packing effects.

The palladium complex **3** crystallizes with a dimethyl sulfoxide solvate molecule. A perspective view of [Pd(4MeOAp4Me$_2$)]$_3$·DMSO with the atomic numbering scheme is shown in Figure 3. The crystallographic data are summarized in Table 2 and selected bond lengths and angles are listed in Table 3 and Table 4, respectively. The core of **3** consists of a six-membered ring of alternating Pd^{II} and S atoms in a chair-like configuration. The remaining two sites of each square planar Pd^{II} center are occupied by the imine nitrogen and the phenoxy oxygen. The dianionic, tridentate ligand has a *ZEZ* configuration about the bonds C1–C6, N1–C8 and N2–C10 for the oxygen, nitrogen and sulfur donor centers. The whole structure forms into a type of bowl with the (3Pd–3S) ring as the base. The bowl almost has a non-crystallographic threefold symmetry except for the disposition of the methoxyphenyl group, C(7)–O(2), on the rim. This type of core has been reported previously for palladium complexes.[14] The dihedral angles between the planes of the two chelate rings (Pd–S–C–N–N) **A** and (Pd–N–C–C–O) **B** are 8.73(13), 0.58(15) and 4.39(17)° for Pd1,

Table 4. Selected bond angles (°) for $H_2$4MeOAp4Me$_2$ and [Pd(4MeOAp4Me$_2$)]$_3$·DMSO

$H_2$4MeOAp4Me$_2$		[Pd(4MeOAp4Me$_2$)]$_3$·DMSO	
N3–C10–S1	126.6(12)	N3–C10–S1	118.4(4)
N2–C10–S1	121.2(12)	N2–C10–S1	122.8(4)
N2–C10–N3	112.1(14)	N2–C10–N3	118.4(4)
N1–N2–C10	121.4(12)	N1–N2–C10	115.9(4)
C8–N1–N2	121.1(11)	C8–N1–N2	114.8(4)
O1–C1–C2	110.6(13)	O1–C1–C2	116.8(4)
N6–C22–S2	122.2(11)	N6–C22–S2	117.1(3)
N5–C22–S2	122.1(11)	N5–C22–S2	122.7(4)
N5–C22–N6	115.6(12)	N5–C22–N6	117.1(3)
N4–N5–C22	116.8(13)	N4–N5–C22	117.0(4)
C20–N4–N5	115.4(13)	C20–N4–N5	114.1(4)
O3–C13–C18	116.0(12)	O3–C13–C18	125.5(5)
		N9–C34–S3	117.6(3)
		N8–C34–S3	123.2(3)
		N8–C34–N9	117.6(3)
		N7–N8–C34	114.3(4)
		C32–N7–N8	114.3(4)
		O5–C25–C30	125.5(5)
Pd_3 Complex		S1–Pd1–S3	89.97(4)
C10–S1–Pd1	95.23(17)	S1–Pd1–O1	178.91(11)
C10–S1–Pd2	104.93(13)	S3–Pd1–O1	91.10(10)
C22–S2–Pd2	95.15(18)	S3–Pd1–N1	172.91(11)
C22–S2–Pd3	103.53(16)	S1–Pd2–S2	92.26(4)
C34–S3–Pd3	96.17(13)	S1–Pd2–O3	89.21(10)
C34–S3–Pd1	101.31(15)	S2–Pd2–O3	176.23(11)
C1–O1–Pd1	122.4(3)	S2–Pd2–N4	85.47(13)
C13–O3–Pd2	125.5(3)	S2–Pd3–S3	90.69(4)
C25–O5–Pd3	123.9(3)	S2–Pd3–O5	90.33(11)
C8–N1–Pd1	125.7(3)	S3–Pd3–O5	178.86(12)
C20–N4–Pd2	119.5(3)	S3–Pd3–N7	85.54(11)
C32–N7–Pd3	125.4(3)	Pd1–S1–Pd2	95.29(4)
N2–N1–Pd1	118.4(3)	S1–Pd1–N1	85.64(11)
N5–N4–Pd2	119.5(3)	Pd2–S2–Pd3	104.18(5)
N8–N7–Pd3	116.1(4)	O1–Pd1–N1	93.27(14)
		Pd1–S3–Pd3	98.43(4)
		S1–Pd2–N4	176.27(12)
		S2–Pd3–N7	175.79(11)
		O3–Pd2–N4	93.24(16)
		O5–Pd3–N7	93.42(15)

Table 5. Distances (Å) and angles (°) for the inter- and intramolecular hydrogen bonding in $H_2$4MeOAp4Me$_2$ and [Pd(4MeOAp4Me$_2$)]$_3$·DMSO

Donor, D	H	Acceptor, A[a]	D···A	H···A	D–H···A
$H_2$4MeOAp4Me$_2$					
O1	H1	N1	2.58(2)	2.00(1)	115.1(8)
O3	H3	N4	2.53(2)	1.68(1)	139.4(7)
O1	H1	S1	3.69(2)	2.71(3)	167.2(7)
O3	H3	S2	3.60(2)	2.76(3)	139.4(7)
N2	H2	S2i	3.65(2)	3.405(3)	98.5(9)
N5	H5	S1i	3.70(2)	3.468(3)	97.7(9)
C(12)	H(12B)	O(3)ii	3.40(2)	2.550(1)	149.2(7)
[Pd(4MeOAp4Me$_2$)]$_2$·DMSO					
C17	H17A	O7i	3.491(7)	2.598(4)	156.7(3)
C19	H19A	O2ii	3.235(7)v	2.546(4)	127.4(3)
C38	H38A	O6iii	3.385(9)	2.488(4)	152.0(4)
C31	H31B	O7a	3.526(8)	2.569(5)	165.5(4)
C36	H36C	S3	3.027(4)	2.5670(11)	102.8(2)
C23	H23C	S2	3.087(6)	2.5816(12)	112.2(3)
C33	H33A	N8	2.649(6)	2.253(4)	102.8(3)
C–H..Cg[b]			H..Cg	X..Cg	C–H..Cg
C5–H5B→ Cg3i			3.020	3.757	135.50
C7–H7B→ Cg6ii			3.225	3.994	126.72
C9–H9A→ Cg1iii			2.698	3.324	122.19
C9–H9B→ Cg1iii			3.196	3.324	88.86
C24–H24A→ Cg9iv			3.277	3.869/P'	120.59
C29–H29A→ Cg9v			2.875	3.752/P'	154.18
C37–H37A→ Cg6iv			2.987	3.691/P'	129.77

[a] Symmetry operations: i: 1 – *x*, 2 – *y*, –*z*; ii: *x*, 1 + *y*, *z*; iii: 1 – *y*, –*z*. – [b] Symmetry operations: i: –1 + *x*, *y*, *z*; ii: –1 + *x*, –1 + *y*, *z*; iii: –*x*, 2 – *y*, 1 – *z*; iv: 1 + *x*, *y*, *z*; v: *x*, –1 + *y*, *z*. Cg1 and Cg3 are referred to the centroids Pd1–S1–C10–N2–N1 and Pd3–S3–C34–N7–N8, respectively, and Cg6 and Cg9 are referred to the centroids Pd2–N4–C20–C18–C13–O3 and C13–C14–C15–C16–C17–C(18), respectively.

Pd2 and Pd3, respectively, indicating that there is some deviation from planarity by the ligands. The plane **A** of Pd1 is tilted by 83.46(14) and 73.58(14)° with respect to the plane **A** of Pd2 and Pd3, respectively.

The distances between the palladium centers [Pd1–Pd2, 3.4118(5) Å; Pd2–Pd3, 3.4746(5) Å; and Pd1–Pd3, 3.6528(5) Å] indicate that there is no direct bond between the palladium atoms. However, a very weak interaction can be postulated in agreement with the reported values for polynuclear palladium complexes [2.549(2)–3.539(1) Å].[3][8][15] The three bond angles involving bridging sulfur atoms are as follows: Pd1–S1–Pd2, 95.29(4)°; Pd2–S2–Pd3, 104.18(5)°; Pd1–S3–Pd3, 98.43(4)°. The Pd–N bond lengths range from 2.004(4) to 2.012(4) Å, the Pd–O distances from 1.987(4) to 2.000(3) Å, and the Pd–S distances from 2.2536(12) to 2.3579(12) Å and are similar to those found in other palladium complexes.[8][10] The greater *trans* influence of the iminic nitrogens can be observed in the lengthening of the *trans* Pd–S distances [2.3579(12)–2.3347(13) Å] with respect to the Pd–S distances *trans* to the phenoxy oxygens [2.2536(12)–2.2713(12) Å]. A comparison of the palladium-donor atom and thiosemicarbazonato moiety bond lengths of **3** and a related palladium complex[8] is shown in Table 6. The negative charge of the dianionic ligand is delocalized over the thiosemicarbazonato moiety and the S–C bond lengths are consistent with increased single bond character, while the imine C–N distances and both thioamide C–N distances indicate considerable double bond character.

The C–S bond length increases from an average of 1.68(2) Å in $H_2$4MeOAp4Me$_2$ to an average of 1.803(5) Å in **3** consistent with this bond's change from a conventional double bond to a single bond. Coordination of the imine nitrogen and phenoxy oxygen causes much smaller changes in the C–N and C–O bond lengths. The thioamide C–N bond (e.g., N2–C10), which formally changes from a single bond to a double bond on coordination, decreases from an average of 1.37(2) Å in $H_2$4MeOAp4Me$_2$ to 1.299(7) Å in **3**. The other thiosemicarbazone bonds' average distances also undergo modest changes on coordination, but the changes are not more than three times the combination of the estimated standard deviations of the bonds in the two compounds. The average bond angles also change on coordination to the palladium centers with most bond angles in the thiosemicarbazone moiety and the phenoxy function increasing or decreasing by at least 5°.

The dimethyl sulfoxide molecule appears to be linked via a three-center hydrogen bond (i.e., bifurcated). This bifurc-

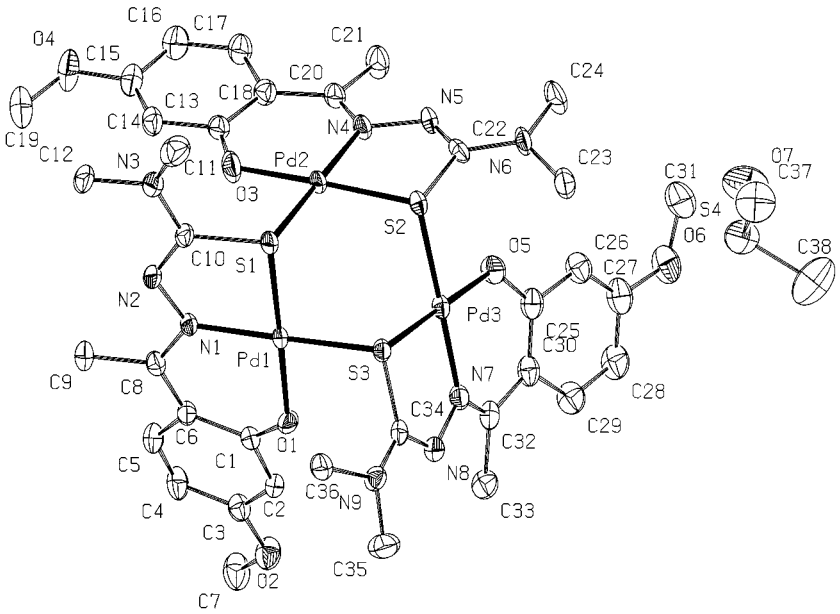

Figure 3. Structural representation of $[Pd(4MeOAp4Me_2)]_3$·DMSO with the labeling scheme; hydrogen atoms are omitted

Table 6. Comparison of bond lengths of trinuclear palladium complexes of 2-hydroxyacetophenone N^4-substituted thiosemicarbazones

Mode	$[Pd(Ap4E)]_3$·DMF[a]	$[Pd(MeOAp4Me_2)]_3$·DMSO[b]
C–S	1.797(7)	1.800(6)
	1.798(8)	1.821(4)
	1.788(6)	1.794(5)
C(S)–NR_2	1.343(9)	1.358(6)
	1.33(1)	1.362(6)
	1.33(1)	1.356(5)
N=C(S)	1.291(9)	1.309(7)
	1.304(8)	1.275(6)
	1.293(9)	1.306(6)
N–N	1.400(8)	1.401(5)
	1.406(8)	1.406(6)
	1.395(8)	1.419(5)
C–O	1.30(1)	1.323(5)
	1.309(9)	1.314(5)
	1.312(9)	1.322(6)
N1=C8	1.314(9)	1.316(6)
	1.306(8)	1.316(6)
	1.296(9)	1.334(6)
Pd–S	2.226(2) 2.332(2)	2.2585(12) 2.3347(13)
	2.250(2) 2.315(2)	2.3578(12) 2.2713(12)
	2.231(2) 2.337(2)	2.3579(12) 2.2536(13)
Pd–O	1.967(5)	2.000(3)
	1.993(5)	1.987(4)
	1.994(6)	1.997(3)
Pd–N	2.005(6)	2.012(4)
	2.002(6)	2.004(4)
	2.020(5)	2.004(4)

[a] Ref.[6], where Ap4E is the dianion of 2-hydroxyacetophenone N^4-ethylthiosemicarbazone. – [b] This work.

ated hydrogen bond involves O7 on dimethyl sulfoxide and the hydrogens on the carbon atom of one trimer, C17···H17A, as well as C31′···H31B′ of an adjacent trimer.[13] Further C–H π interactions[13b] and intramolecular bonds stabilize this structure. Although it is remarkable that there are many contacts, and of different types, the interactions themselves are consistent with the known guidelines for hydrogen bond formation.[13c] For $[Pd(MeOAp4Me_2)]_3$·DMSO, molecular recognition of the hydrogen bonds leads to aggregation and a supramolecular assembly. These interactions are listed in Table 6 and are shown in the packing diagram in Figure 4. The high effective charge on methoxy oxygen atoms and on the sulfoxide oxygen atom help to rationalize the extended network of hydrogen bonding contacts in **3**.

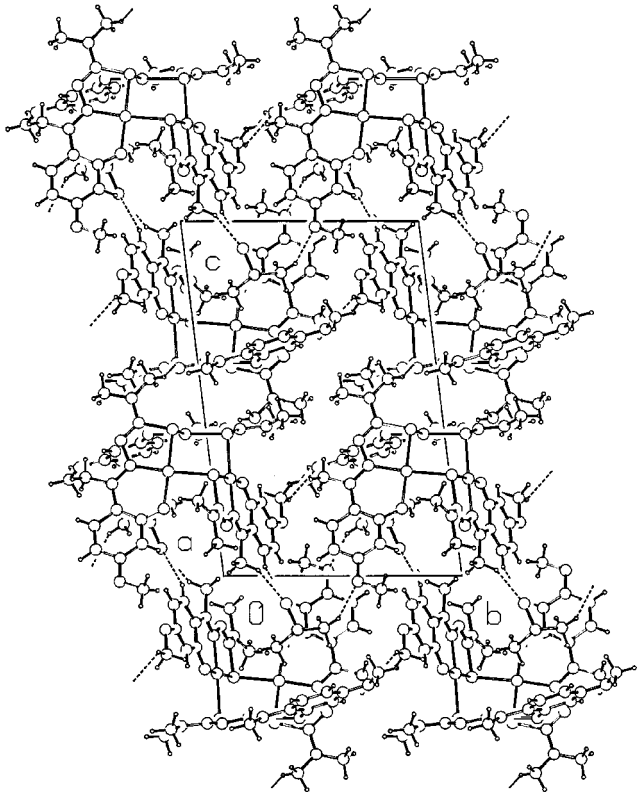

Figure 4. A view of the extended network of the intermolecular hydrogen bonds in $[Pd(4MeOAp4Me_2)]_3$·DMSO along the *a* axis

Spectroscopy

The significant IR bands of $H_2$4MeOAp4Me$_2$ and the three forms of the palladium(II) complex are close in energy to those found in other compounds with tridentate coordination.[9][16] The bands assigned in the spectrum of $H_2$4MeOAp4Me$_2$ shift in the spectrum of the palladium complexes as follows: ν(C=N), from 1556 cm^{-1} to 1541 cm^{-1}; ν(NN), from 1026 cm^{-1} to 1089 cm^{-1}; and ν(CS) (i.e., thioamide IV), from 836 cm^{-1} to 787 cm^{-1}. The palladium-donor atom stretching frequencies are as follows: ν(PdN, imine), 511 cm^{-1}; ν(PdS), 387 cm^{-1}; and ν(PdO), 338 cm^{-1}. Complex **2** exhibits a broad band at 3400 cm^{-1} attributed to the presence of lattice water. The DMSO adduct **3** shows a very strong S–O stretching vibration at 1023 cm^{-1}. This frequency is lower than that for free DMSO (1100–1055 cm^{-1}), suggesting the interaction of DMSO with the trimer complex through oxygen[16] as detailed above.

The main differences between the ^{1}H NMR spectrum of the free $H_2$4MeOAp4Me$_2$ and the trimer complexes are the disappearance of the downfield O1H (and O3H and N2H and N5H) signals. These changes confirm that loss of both hydrogens and metallation occurs, and that the structure of the complex in the solid state persists in $(CD_3)_2SO$ and $CDCl_3$ solutions. The appearance of the OH peak downfield at δ = 13.191 and 12.525 in $(CD_3)_2SO$ and $CDCl_3$, respectively, for $H_2$4MeOAp4Me$_2$ indicates that OH is hydrogen-bonded to $(CD_3)_2SO$ and intramolecularly hydrogen-bonded to the imine nitrogen N1 (and N4) in $CDCl_3$. The position for N2H (and N5H) is downfield at δ = 9.780 and 10.962 in $(CD_3)_2SO$ and $CDCl_3$, respectively, suggesting that this proton is also involved in hydrogen bonding, with more interaction of this proton in $CDCl_3$ solution.[16b] This suggests that a tautomer may exist in solution, similar to that found in 2-acetylpyridine N^4-substituted thiosemicarbazones,[17] and more recently in 2-pyridineformamide N^4-thiosemicarbazones.[18] This would involve N2H (and N5H) shifting to N1 (and N4) to form a bifurcated hydrogen bond with the phenoxy oxygen and thione sulfur.

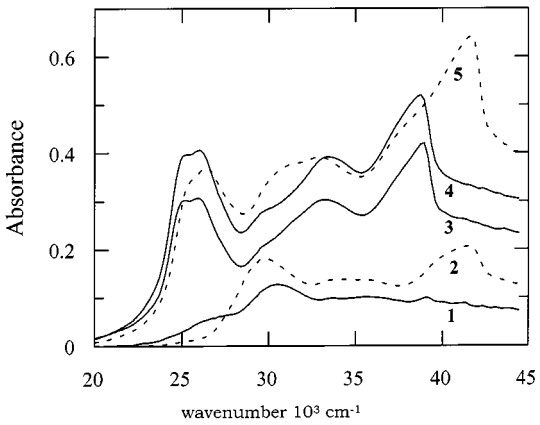

Figure 5. Electronic absorption spectra of $H_2$4MeOAp4Me$_2$; in DMSO (1); in $CHCl_3$ (2); of [Pd(4MeOAp4Me$_2$)]$_3$·3H_2O in DMSO (3); of [Pd(4MeOAp4Me$_2$)]$_3$ in DMSO (4) and of [Pd(4MeOAp4Me$_2$)]$_3$·3H_2O in $CHCl_3$ (5)

The bands of the $H_2$4MeOAp4Me$_2$ at ca. 30000 and 33500 cm^{-1} in the UV/Vis spectrum are due to n → π* transitions of the imine portion of the TSC moiety, and the aromatic ring, respectively.[19] The energies of these two bands are affected by changes in organic solvents due to differences in the mode of hydrogen bonding. The electronic spectrum of the trimer is shown in Figure 5 . Three spin-allowed singlet–singlet d → d transitions are predicted in the visible region of square planar complexes of palladium(II). However, strong charge transfer transitions for [Pd(4MeOAp4Me$_2$)]$_3$ interfere and prevent the observation of all the expected bands. The band at ca. 25000 cm^{-1} is intense and is assigned to a HOMO → LUMO transition.

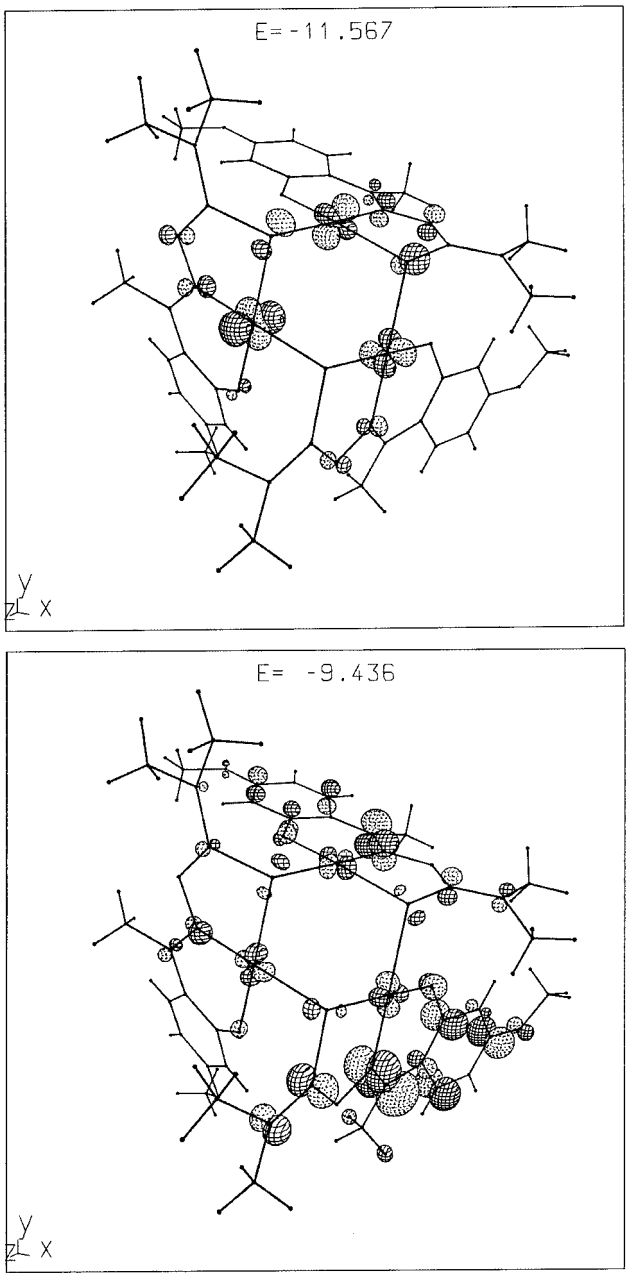

Figure 6. Representation of lowest unoccupied molecular orbital (LUMO: bottom) and highest occupied molecular orbital (HOMO: top) for complex [Pd(4MeOAp4Me$_2$)]$_3$·DMSO

The HOMO and LUMO orbitals are "d"- and π-centered on the metal and on the ligand, respectively. The bands at 25000 and 26000 cm^{-1} are assignable to a combination of d → d and charge transfer transitions.[19] The band at ca. 33000 cm^{-1} is due to the n → π* transition of the thiosemicarbazone moiety (imine, thioamide) and charge transfer involving the TSC moiety (L → M). The maxima at 20000–22000 cm^{-1} and at 26000–28000 cm^{-1} are affected by the nature of the solvent consistent with them having charge-transfer character.

The trinuclear complex was studied by the extended-Hückel method using the CACAO PC Beta-Version 5.0 package.[20] The molecular geometry was established from the crystallographic coordinates of the trinuclear complex. The highest occupied molecular orbital (HOMO; –11.567 eV, Figure 6) is mostly composed of dz2, dxy and dyz and has high percentages of the dz2 (25 %) orbital from Pd1, the dxy (8 %), dyz (10 %) orbitals from Pd2, and dxy (8 %) and dyz (9 %) from Pd3; the lowest unoccupied orbital (LUMO; –9.436 eV, Figure 6) is mostly composed of px orbitals from C32 (–18%), C29 (5%) and N7 (9%). The HOMO's energy is well isolated, strongly suggesting that the assignment of the lowest energy electronic transition can unambiguously be assigned to the computed HOMO–LUMO. This is experimentally addressed. The HOMO–n (n = 1–10) levels are similar in energy, and are more stabilized by ca. 0.5 eV relative to the HOMO. The molecular orbital $HOMO_{-10}$ has components of dxz (20%) from Pd1, dyz (–5%) from Pd2 and p (π) atomic orbitals from N2, N3, N1, C6. This is consistent with a back donation from the metal to π* orbitals from the ligand moieties.[19d]

Experimental Section

General: Solvents were purified and dried according to standard procedures. The palladium(II) complexes were analyzed for C, H and N at the European Environmental Research Institute (Ioannina). Infrared and far-infrared spectra were recorded with a Perkin–Elmer Spectrum GX FT-IR spectrophotometer using KBr (4000–400 cm^{-1}) and polyethylene pellets (400–40 cm^{-1}). Electronic spectra were recorded on a JASCO V-570 spectrophotometer UV/Vis/NIR.

Preparation of the Compounds: 2-Hydroxy-4-methoxyacetophenone N^4-dimethylthiosemicarbazone ($H_2$4MeOAp4Me_2), was prepared by stirring at room temperature a 1:1 ethanol solution (50 mL) of 2-hydroxy-4-methoxyacetophenone (0.05 mol) and N^4-dimethylthiosemicarbazide (0.05 mol) with 3 drops of conc. H_2SO_4 added. N^4-dimethylthiosemicarbazide was prepared following the procedure described by Scovill.[21] The complex Pd(4MeOAp4Me_2)]$_3$·3H_2O (**1**) was prepared directly from the reaction of K_2PdCl_4 (0.392 g, 1.2 mmol) in H_2O (5 mL) and $H_2$4MeOAp4Me_2 (0.267 g, 1 mmol) in CH_3OH (5 mL), with the pH adjusted to ca. 9 with a few drops of a 1.5 M NH_3 solution. After stirring for 24 h at room temperature, the resulting brown powder was filtered off, washed with cold methanol and ether and dried in vacuo over silica gel (yield 70%). – [Pd(MeOAp4Me_2)]$_3$·3H_2O (1169.14): calcd. C 36.98, H 4.39, N 10.78, S 8.23; found C 36.80, H 4.27, N10.95, S 8.40. – Compound **2** was obtained by drying the trihydrate at 40° C initially, and finally at 80° C for 1 h over P_4O_{10} to afford the dehydrated complex [Pd(MeOAp4Me_2)]$_3$. – **2** (1017.07): calcd. C 38.78, H 4.04, N 11.30, S 8.63; found C 38.90, H 4.00, N 11.20, S 8.73. – Slow evaporation of **1** from dimethyl sulfoxide solution yielded dark red crystals of the complex [Pd(MeOAp4Me_2)]$_3$·DMSO (**3**) suitable for X-ray structural analysis. – **3** (1193.40): calcd. C 38.25, H 4.30, N 10.56, S 10.75; found C 38.30, H 4.35, N 10.48, S 10.60.

Crystal Structure Determination of H24MeOAp4Me2 and Complex 3: Crystals of $H_2$4MeOAp4Me_2 were grown by slow concentration of a 1:1 by volume mixture of anhydrous ethanol/acetone and the selected crystal mounted on a glass fiber and used for data collection on a Nonius MACH3 diffractometer. The structure was solved by direct methods[22a] that revealed the positions of all non-hydrogen atoms, and refined on F by a full-matrix least-squares procedures using anisotropic displacement parameters.[22b] The hydrogens attached to nitrogen and oxygen were located by difference Fourier maps and were refined isotropically (U_{iso} = 0.05 Å^2). The remaining hydrogens were located in their calculated positions (C–H 0.96 Å). – A red needle-like crystal, (ca. 0.02 × 0.04 × 0.40 mm) of **3** was mounted on a glass fiber and analyzed with a Bruker SMART 1 K CCD diffractometer equipped with an Oxford Cryosystems Cryostream cooler,[23a] running at 123 K. The data collection nominally covered a sphere of reciprocal space by a combination of five sets of exposures; each exposure set had a different φ angle for the crystal and each exposure covered 0.3° in ω in 30 s. The crystal-to-detector distance was 4.909 cm. Coverage of the unique set was over 98% complete to φ = 26.37° (data truncated at 0.80Å). Data reduction was performed with the program SAINT V4.05.[23b] Crystal decay was monitored by repeating the first 50 frames of data at the end of data collection and analyzing the duplicate reflections. Area detector scaling and absorption corrections were performed by SADABS.[23b] This correction was used to scale the frames of data and to correct for absorption of the primary beam by the crystal support using the method of Blessing.[23c] A correction for absorption of the primary beam by the crystal was not applied. All calculations were performed with SHELXTL.[23d] Crystallographic data for $C_{36}H_{45}N_9O_6Pd_3S_3·C_2H_6OS$ (CCDC-132172) and $C_{12}H_{17}N_3O_2S$ (CCDC-132400) have been deposited with the Cambridge Crystallographic Data Centre. Copies of available material can be obtained, free of charge, on application to CCDC, 12 Union Road, Cambridge CB2 1EZ, UK [Fax: (internat.) + 44-1223/336-033; E-mail: deposit@ccdc.cam.ac.uk].

Calculations: A computational study with a PM3 parameterization scheme[11a] utilizing the eigenvector-following algorithm,[11b] as implemented in the MOPAC93 program,[11c] was used to investigate the prevailing isomer of free $H_2$4MeOAp4Me_2, the monodeprotonated anion, H4MeOAp4Me_2^-, and the diprotonated anion, 4MeOAp4Me_2^{2-}, in the gas phase and simulated solvent bulk (COSMO model[11d]). The complex molecule **3** was studied by the extended-Hückel method using the CACAO PC Beta-Version 5.0 package. The crystallographic coordinates of the complex were used.[20]

[1] Tsuji, *Organic Synthesis with Palladium Compound*, Springer-Verlag, New York, **1980**; R. F. Heck, *Palladium Reagents in Organic Synthesis*, Academic Press, London, **1985**.
[2] [2a] G. W. Parshall, S. D. Ittel, *Homogeneous catalysis*, 2nd ed., Wiley, New York, **1992**. – [2b] F. A. Cotton, S. Han, *Rev. Chim. Miner.* **1983**, 496. – [2c] F. A. Cotton, S. Han, *Rev. Chim. Miner.* **1985**, 277. – [2d] D. H. R. Barton, J. Khamsi, N. Ozbalik, M. Ramesh, J. Sharma, *Tetrahedron* **1989**, *30*, 4661.
[3] [3a] A. C. Skapski, M. Smart, *J. Chem. Soc., Chem. Commun.* **1970**, 658. – [3b] M. Basato, A. Grassi, G. Valle, *Organometallics* **1995**, *14*, 4439. – [3c] A. Deeming, M. N. Meah, P.A. Beates, M.B. Hursthouse, *J. Chem. Soc., Dalton Trans.* **1988**, 2193. – [3d] M. Sommovigo, M. Pasquali, F. Marchetti, P. Leoni, T.

Beringhell, *Inorg. Chem.* **1994**, *33*, 2651. – [3e] M. Parra-Hake, M. F. Retting, R. M. Wing, *Organometallics* **1983**, *2*, 1013. – [3f] P. M. Bailey, A. Kelly, P.M. Maitlis, *J. Chem. Soc., Dalton Trans.* **1978**, 1825. – [3g] M. Basato, C. Bertani, B. Sesto, M. Zecca, A. Grassi, G. Valle, *J. Organometallic Chem.* **1998**, *552*, 277. – [3h] M. Basato, D. Tommasi, M. Zecca, *J. Organometall. Chem.* **1998**, *571*, 115.

[4] D. X. West, S. B. Padhye, P. B. Sonawane, R. C. Chikate, *Asian J. Chem. Rev.* **1990**, *1*, 125.

[5] D. E. Barber, Z. Lu, T. Richardson, R. H. Crabtree, *Inorg. Chem.* **1992**, *31*, 4709.

[6] D. X. West, Y-H. Yang, T. L. Klein, K. I. Goldberg, A. E. Liberta, J. Valdés-Martínez, R. A. Toscano, *Polyhedron* **1995**, *14*, 1681.

[7] D. X. West, Y-H. Yang, T. L. Klein, K. I. Goldberg, A. E. Liberta, J. Valdés-Martínez, S. Hernández-Ortega, *Polyhedron* **1995**, *14*, 3051.

[8] D. Kovala-Demertzi, N. Kourkoumelis, D. X. West, J. Valdés-Martínez, S. Hernández-Ortega, *Eur. J. Inorg. Chem.* **1998**, 861.

[9] A. Berkessel, G. Hermann, O-T. Racuch, M. Buchner, A. Jacobi, G. Huttner, *Chem. Ber.* **1996**, *129*, 1421.

[10] [10a] A. Papageorgiou, Z. Iakovidou, D. Mourelatos, E. Mioglou, L. Boutis, A. Kotsis, D. Kovala-Demertzi, A. Domopoulou, D. X. West, M. A. Demertzis, *Anticancer Res.* **1997**, *17*, 247. – [10b] D. Kovala-Demertzi, A. Domopoulou, M. A. Demertzis, A. Papageorgiou, D. X. West, *Polyhedron* **1997**, *16*, 3625. – [10c] D. Kovala-Demertzi, A. Domopoulou, G. Valle, M. A. Demertzis, A. Papageorgiou, *J. Inorg. Biochem.* **1997**, *68*, 147. – [10d] D. Kovala-Demertzi, M. A. Demertzis, V. Varagi, A. Papageorgiou, D. Mourelatos, E. Mioglou, Z. Iakovidou, A. Kotsis, *Chemotherapy* **1998**, *44*, 421.

[11] [11a] J. J. P. Stewart, *J. Comput. Chem.* **1989**, *10*, 210. – [11b] J. Baker, *J. Comput. Chem.* **1986**, *7*, 385. – [11c] J. J. P. Stewart, *MOPAC93*, Fujitsu Co., **1993**. – [11d] A. Klamt, G. Shurmann, *J. Chem. Soc., Perkin Trans.* **1993**, 799.

[12] J. Valdés-Martínez, S. Hernández-Ortega, D. X. West, L. J. Ackerman, J. K. Swearingen, A. K. Hermetet, *J. Mol. Struct.* **1999**, *478*, 219.

[13] [13a] T. Steiner, B. Lutz, J. van der Maas, A. M. M. Schreurs, J. Kroon, M. Tamm, *Chem. Commun.* **1998**, 171. – [13b] T. Steiner, M. Tamm, A. Grzegorzewski, N. Schulte, N. Veldman, A. M. M. Schreurs, J. Kroon, J. van der Maas, B. Lutz, *J. Chem. Soc., Perkin Trans. 2* **1996**, 2441. – [13c] M. C. Etter, *Acc. Chem. Res.* **1990**, *23*, *120*. – [13d] T. Steiner, *Cryst. Rev.* **1996**, *6*, 1.

[14] [14a] M. Yasui, S. Yoshida, S. Kakuma, S. Shimamato, N. Matsumura, F. Iwasaki, *Bull. Chem. Soc. Jpn.* **1996**, *69*, 2749. – [14b] J. P. Fackler Junior, W. J. Zegarski, *J. Am. Chem. Soc.* **1973,** *95*, 8566. – [14c] Kang-Woo Kim, M.G. Kanatzidis, *J. Am. Chem. Soc*. **1995**, *117*, 5606.

[15] A. G. Quiroga, J. M. Pärez, I. Lopez-Solera, J. R. Masaguer, A. Luque, P. Roman, A. Edwards, C. Alonso, C. Navarro-Ranninger, *J. Med. Chem.* **1998**, *41,* 9, 1399.

[16] [16a] D. X. West, M. M. Salberg, G. A. Bain, A. E. Liberta, *Transition Met. Chem.* **1997**, *22*, 180. – [16b] K. Nakamoto, *Infrared and Raman Spectra of Inorganic and Coordination Compounds*, 5th ed., Wiley, New York, 1997.

[17] D. X. West, G. A. Bain, R. J. Butcher, J. P. Jasinski, R. Y. Pozdniakiv, Y. Li, J. Valdés-Martínez, R. A. Toscano, S. Hernández-Ortega, *Polyhedron* **1996**, *15*, 665.

[18] D. X. West, J. K. Swearingen et al., unpublished results.

[19] [19a] D. Kovala-Demertzi, J. M. Tsangaris, H. O. Desseyn, B. J. Van der Veken, *Bull. Soc. Chim. Belg.* **1987**, *1*, 7. – [19b] A. B. P. Lever, *Inorganic Electronic Spectroscopy*, Elsevier, New York, **1984**. – [19c] G. L. Estiu, A. H. Jubert, J. Costamagna, J. Vargas, *Inorg. Chem.* **1996**, *35*, 263. – [19d] D. Di Leo, F. Berrettini, R. Cini, *J. Chem. Soc., Dalton Trans.* **1998**, 1993.

[20] C. Mealli and D. Proserpio, CACAO PC Beta-Version 5.0, **1998**; C. Mealli, D. Proserpio, *J. Chem. Educ.* **1990**, *11*, 440.

[21] J. P. Scovill, *Phosphorus Sulfur Silicon* **1991**, *60*, 15.

[22] [22a] A. Altomere, G. Cascarano, C. Giacovazzo, A. Guagliardi, M. C. Burla, G. Polidori and M. Camalli, *J. Appl. Crystallogr.* **1994**, *27*, 435. – [22b] S. Mackay, C. Edwards, A. Henderson, C. Gilmore, N. Steward, K. Shankland, A. Donald, University of Glasgow, Scotland, **1997**. – [22c] A. L. Spek, *PLATON: A program for the automated generation of a variety of geometrical entities*, University of Utrecht, The Netherlands, **1997**.

[23] [23a] J. Cosier and A. M. Glazer, *J. Appl. Crystallogr.* **1986**, *19*, 105. – [23b] Bruker AXS Inc., *SMART, SAINT and SADABS Area-detector control and integration software Version 4.*, Bruker AXS Inc., Madison WI 53719, U.S.A., **1998**. – [23c] R. H. Blessing, *Acta Crystallogr., Sect. A* **1995**, *A51*, 33. – [23d] G. M. Sheldrick, *SHELXTL Version 5.10.*, Bruker AXS Inc., Madison, WI 53719, U.S.A, **1998**.

Received August 4, 1999
[I99287]